Carbohydrate Polymers 323 (2024) 121360

Contents lists available at ScienceDirect

Carbohydrate Polymers

journal homepage: www.elsevier.com/locate/carbpol

Addressing the complexities in measuring cyclodextrin-sterol binding constants: A multidimensional study

Amelia M. Anderson [a,b,c,1], Ilse Manet [d,1], Milo Malanga [e,f], Daniel M. Clemens [a], Keivan Sadrerafi [a], Ángel Piñeiro [b,g], Rebeca García-Fandiño [c,g], Matthew S. O'Connor [a,*]

[a] Cyclarity Therapeutics, 8001 Redwood Blvd Novato, CA 94945, USA
[b] Departamento de Física Aplicada, Facultade de Física, Universidade de Santiago de Compostela, E-15782 Santiago de Compostela, Spain
[c] Departamento de Química Orgánica, Centro Singular de Investigación en Química Biolóxica e Materiais Moleculares (CiQUS), Universidade de Santiago de Compostela, Campus Vida s/n, E-15782 Santiago de Compostela, Spain
[d] Istituto per la Sintesi Organica e la Fotoreattività (ISOF), Consiglio Nazionale delle Ricerche (CNR), via P. Gobetti 101, Bologna 40129, Italy
[e] CarboHyde, Budapest, Berlini u. 47-49, 1045, Hungary
[f] Cyclolab Cyclodextrin Research and Development Ltd., Budapest, Illatos út 7 1097, Hungary
[g] MD.USE Innovative Solutions S.L., Edificio Emprendia, Campus Vida, Santiago de Compostela, Spain

ARTICLE INFO

Keywords:
Cyclodextrin
Inclusion complex
Affinity constant
Circular dichroism
Isothermal titration calorimetry
Metadynamics simulations

ABSTRACT

A class of cyclodextrin (CD) dimers has emerged as a potential new treatment for atherosclerosis; they work by forming strong, soluble inclusion complexes with oxysterols, allowing the body to reduce and heal arterial plaques. However, characterizing the interactions between CD dimers and oxysterols presents formidable challenges due to low sterol solubility, the synthesis of modified CDs resulting in varying number and position of molecular substitutions, and the diversity of interaction mechanisms. To address these challenges and illuminate the nuances of CD-sterol interactions, we have used multiple orthogonal approaches for a comprehensive characterization. Results obtained from three independent techniques - metadynamics simulations, competitive isothermal titration calorimetry, and circular dichroism - to quantify CD-sterol binding are presented. The objective of this study is to obtain the binding constants and gain insights into the intricate nature of the system, while accounting for the advantages and limitations of each method. Notably, our findings demonstrate ~1000× stronger affinity of the CD dimer for 7-ketocholesterol in comparison to cholesterol for the 1:1 complex in direct binding assays. These methodologies and findings not only enhance our understanding of CD dimer-sterol interactions, but could also be generally applicable to prediction and quantification of other challenging host-guest complex systems.

1. Introduction

Cyclodextrins (CDs) are cyclic carbohydrates composed of 6, 7, or 8 glucose residues, denoted as αCD, βCD, and γCD, respectively (Kurkov & Loftsson, 2013). Although traditionally depicted as rigid, truncated conical structures, CDs exhibit considerable flexibility, not only in solution but also in solid state (Dodziuk, 2002). These molecules are typically simplified as a hydrophobic cavity encased within a hydrophilic shell, enabling CDs to encapsulate and solubilize hydrophobic guest molecules, such as cholesterols, in aqueous environments through the formation of inclusion complexes (Cai et al., 2009; Christoforides et al., 2018; Yu et al., 2006). CDs have a narrow side (tail) and a wide side (head) that can be chemically modified by substituting some hydroxyls with other functional groups such as hydroxypropyl (HP) or methyl, which can significantly enhance their solubility and change their properties in a variety of ways (Jabbari & Sadeghi, 2012; Kurkov & Loftsson, 2013; Loftsson et al., 2019; Varan et al., 2017). CDs are in wide use for industrial and drug delivery applications and have an excellent

Abbreviations: CD, cyclodextrin; API, active pharmaceutical ingredient; CHOL, cholesterol; 7KC, 7-ketocholesterol; PMF, potential of mean force; ITC, isothermal titration calorimetry; CiDi, circular dichroism; COM, center of mass; CV, collective variable; RAMEB, randomly methylated βCD monomers; MD, molecular dynamics; DS, degree of substitution; HP, 2-hydroxypropyl; GPU, glucopyranoside unit; DIC, double inclusion complex; HPβCD, hydroxypropyl-β-cyclodextrin.

* Corresponding author.
E-mail address: matthew.oconnor@cyclaritytx.com (M.S. O'Connor).

[1] AMA and IM contributed equally to this work.

https://doi.org/10.1016/j.carbpol.2023.121360
Received 24 July 2023; Received in revised form 22 August 2023; Accepted 30 August 2023
Available online 9 September 2023

safety profile (Schmid, 2001); when used in medicine, CDs are usually employed as excipients and are not considered pharmaceutically active themselves. There are two notable exceptions to this: Bridion™, a CD API (active pharmaceutical ingredient) drug widely approved and used for reversal of neuromuscular block during surgical procedures (Merck and Co, Inc., 2015), and clinical trials are being conducted using Hydroxypropyl-β-cyclodextrin (HPβCD) to treat Niemann Pick Type C disease, a debilitating disease of cholesterol metabolism, (Safety and Efficacy of Intravenous Trappsol Cyclo (HPBCD) in Niemann-Pick Type C Patients, n.d.), however with serious side effects due to the incredibly high doses of monomer necessary (Puglisi & Yagci, 2019). Both of these APIs take advantage of CDs forming inclusion complexes with target molecules, and it has been shown that CD dimers can further enhance the solubility of CHOL in water (Alcalde et al., 2009; Anderson et al., 2021; Breslow & Zhang, 1996).

The crystal structure of the inclusion complex of cholesterol in unsubstituted βCD monomers reveals CHOL encapsulated inside of a naturally formed (not covalently linked) head-to-head βCD dimer, which has been recapitulated in computational studies (Christoforides et al., 2018; Hayashino et al., 2018; Kučáková & Dolenský, 2020). Other CD dimers have been synthesized for various purposes (Aime et al., 2009; Alcalde et al., 2009; Anderson et al., 2021; Aykaç et al., 2012; Blaszkiewicz et al., 2013; Breslow et al., 1989; Casas-Solvas et al., 2011; Chmurski et al., 2016; de Jong et al., 2000; Lebedinskiy et al., 2022; Shuang et al., 2020). Regarding head-to-head dimers complexing CHOL, corresponding to the crystal structure and NMR structure (Christoforides et al., 2018; Kučáková & Dolenský, 2020), little research has been conducted and sterol solubility remains an issue. The binding affinity of CHOL for linked tail-to-tail CD dimers has been shown to be enhanced due to a chelate effect by phase-solubility (Alcalde et al., 2009; Breslow & Zhang, 1996), but a more reliable method for determining binding constants remains elusive due to the very low aqueous solubility of CHOL.

Recently, Cyclarity Therapeutics has engineered CD dimers as innovative APIs for the treatment of atherosclerosis, a leading cause of cardiovascular diseases (Anderson et al., 2020; Anderson et al., 2021). Current treatments for atherosclerosis primarily focus on managing risk factors and alleviating symptoms (Banach et al., 2016; Katzmann et al., 2020; Strandberg et al., 2020), but it is proposed that CD dimers can effectively reverse arterial plaque formation by specifically encapsulating atherosclerotic and cytotoxic oxysterols (Anderson et al., 2021; Breslow & Zhang, 1996; Coisne et al., 2016; Kritharides et al., 1996; Martinet et al., 2008, Kim et al., 2020). In this case, the challenge lies in selectively encapsulating toxic 7-ketocholesterol (7KC) over essential cholesterol (CHOL), as these sterol molecules only differ by a single heavy atom - an oxygen doubly-bound to carbon 7 - making them difficult to distinguish. Selectivity for 7KC over CHOL is important because CHOL plays a crucial role in maintaining cell membrane integrity, fluidity, and functionality, whereas 7KC is a cytotoxic oxysterol that can contribute to the development of various pathologies, including atherosclerosis (Anderson et al., 2020). This research focuses on CD dimers as they exhibit several advantages over monomers, including their enhanced affinity for encapsulating sterol molecules, and a higher density of functional groups that can be substituted within a single molecule, facilitating the potential for specificity of the modified structure (Anderson et al., 2021; Breslow et al., 1995; Kritharides et al., 1996; Voskuhl et al., 2011). Furthermore, the chemical linker connecting the two CD monomers can be tailored to optimize the recognition and encapsulation of particular ligands (Breslow et al., 1989; Breslow & Zhang, 1996; Chmurski et al., 2016; Liu & Chen, 2006; Shuang et al., 2020; Soto Tellini et al., 2006).

The capacity of a macrocycle to accurately identify and bind to a particular ligand can be quantified in terms of the standard Gibbs energy (ΔG^0) associated with the formation of the resultant supramolecular complex. In general, the change in any macroscopic physical observable as a function of the concentration ratio of the CD and ligand can be used to determine ΔG^0 or, equivalently, the corresponding association/binding constant(s) ($K_A = \exp(-\Delta G^0 / RT)$) (Connors, 1987; Piñeiro et al., 2019). The determination of this parameter is essential to understanding the molecular interactions and to design drugs with improved efficacy and specificity. However, a universal, rapid, precise, and cost-effective approach to measure ΔG^0 values has not yet been developed. Many wet lab-based methods have been proposed for this aim in the field of the CDs, including isothermal titration calorimetry (ITC) (Peluso et al., 2023; Piñeiro et al., 2022), surface plasmon resonance (SPR) (Hayashi et al., 2010), nuclear magnetic resonance (NMR) (Doan et al., 2022), microscale thermophoresis (MST) (Niether et al., 2017), circular dichroism spectrophotometry (CiDi, so as not to be confused with CD for cyclodextrin) (Wankar et al., 2017), fluorescence spectroscopy (Al-Soufi et al., 2008; Anand et al., 2012; Salzano et al., 2017), surface tension (Piñeiro et al., 2007), mass spectroscopy (Jankowski et al., 2016), and capillary electrophoresis (Aksamija et al., 2022; Peluso et al., 2023).

Although numerous methods for measuring K_A and ΔG^0 are available, they exhibit certain limitations for CD dimer-sterol systems, such as the requisite concentration and solubility of the compounds involved, the signal-to-noise ratio, or artifacts associated with sample labeling (Flood et al., 2001; Mura, 2014). The binding constants must also be measured in biologically relevant solvent if they are to be used for drug development, and sterols are highly insoluble in aqueous media. A range of computational methods have been proposed as alternatives to determine ΔG^0 values but, again, none of them provides a universal solution to the problem (Hayashino et al., 2018; López et al., 2011, 2013). The most common issues with these approaches are the production of unrealistic results due to oversimplifications of the studied systems and the excessive consumption of computational resources for obtaining reliable energy values.

Here, we present an orthogonal characterization of the complexes between HPβCD dimers and CHOL or 7KC using one computational and two wet lab methods: computational metadynamics simulations followed by PMF calculations, ITC, and CiDi. Each of these methods has required significant optimization for these kinds of host-guest systems. They provide cooperative insight on the interaction between the CD dimer and the sterol molecules, including energy profiles, optimized structures for the supramolecular complexes and independent quantitative estimations of the corresponding binding affinities. This approach is expected to contribute to the development of novel therapies and other technologies targeting the selective sequestration of small hydrophobic molecules, offering new possibilities for the treatment of ailments involving the accumulation of hydrophobic toxins. Our ultimate goal is to develop CDs as APIs for the treatment and reversal of all cholesterol-related dyslipidemia, but the methodologies presented here could also be applied to a range of complex molecular systems.

Our hypothesis posits that the complexity of CD dimer-sterol inclusion complexes necessitates the integration of multiple methods rather than relying on a single approach. Factors like flexibility, solubility variations, diverse substitutions, and multiple stoichiometries contribute to this complexity, and our multi-method approach illuminates CD dimer-sterol behavior comprehensively. These orthogonal techniques independently estimate K_A and ΔG^0 values, showcasing selective 7KC encapsulation by the CD dimer. This approach underscores how a multidimensional analysis deepens understanding of CD-sterol inclusion complex formation, both qualitatively and quantitatively.

2. Materials

The same HPβCD dimer was used for both ITC and CiDi experiments, custom synthesized by Cyclarity Therapeutics. 98.60 % purity (Fig. 1).

NMR experiments (Figs. S1–S7) were performed using two different spectrometers: a 600 MHz Varian DDR NMR spectrometer equipped with a 5 mm inverse-detection gradient (IDPFG) probehead, and a Bruker Advance III HD 600 MHz spectrometer equipped with a QCI 1H/

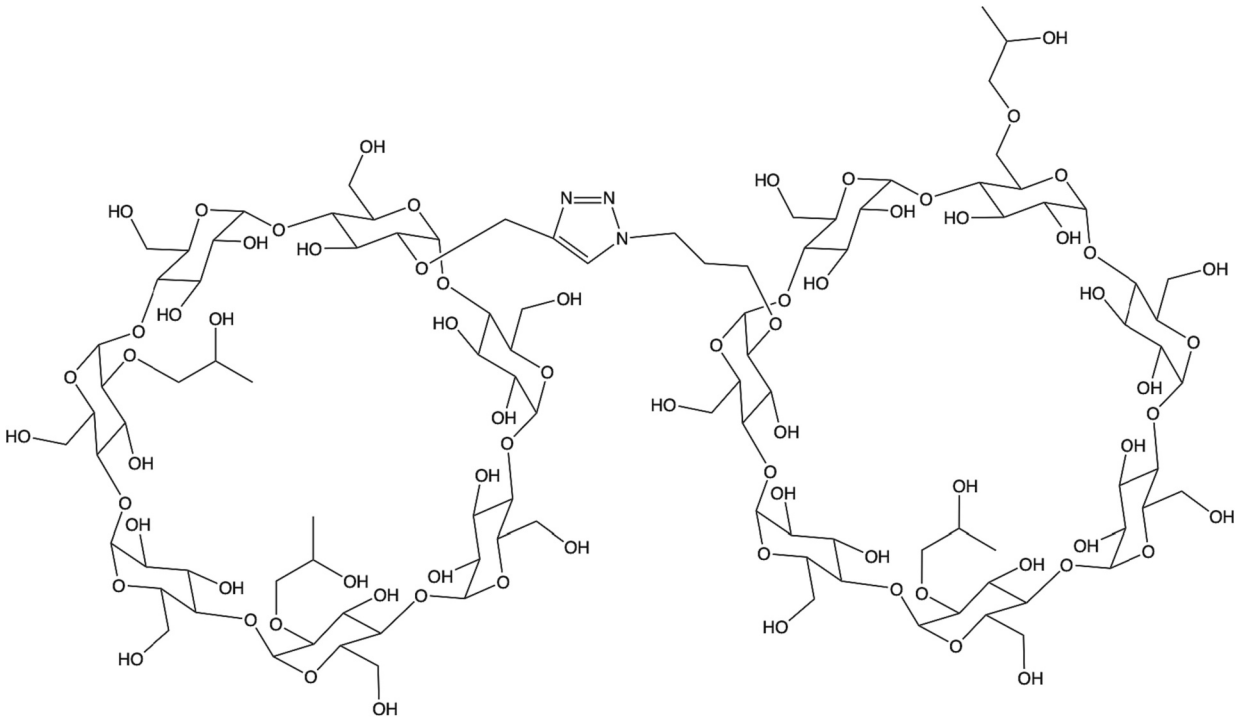

Fig. 1. Structure of the head-to-head HPβCD dimer used for CiDi and ITC. Note that the actual product is an isomeric mixture of HPβCD dimers, this structure represents just one isomer of the HPβCD dimer. The narrow side, or "primary face", is facing outside (where the O6 oxygens reside), while the wide side, or "secondary face", of each CD monomer is facing inside (where the O2 and O3 oxygens reside).

13C/15N/31P proton-optimized quadrupole inverse cryoprobe with 1H and 13C cryochannels. The standard pulse sequences and processing routines available in VnmrJ 3.2 C/Chempack 5.1 or Bruker TopSpin 3.6.2 software were used for structure identifications. The experiments were conducted at a temperature of 298 K using standard 5 mm NMR tubes. Chemical shifts (δ) are reported in parts per million (ppm) and referenced to the residual signals of the NMR solvents: dimethyl sulfoxide-d_6 (δ1H = 1.25 ppm, δ13C = 39.52 ppm) or D2O (δ1H = 4.79 ppm). J values are reported in hertz (Hz). Samples were prepared by dissolving 10 mg of solid in 0.7 mL of deuterated solvent. The identification of the HPβCD dimer using NMR spectroscopy involved cross-linking the data obtained from 1H, 13C, COSY, DEPT-edited HSQC, and HMBC spectra in DMSO-d_6.

The HPβCD dimer is an isomeric mixture of differently substituted βCD dimer core derivatives with varying degrees of substitution (DS). The determination of the average DS was based on ^{1}H NMR measurements in D2O (Figs. S2–3). The signals in the anomeric region (4.9–5.3 ppm) were integrated together and set to be 14.00. The methyl signal at 1.08 ppm was then divided by three to calculate the average number of 2-hydroxypropyl units on the HPβCD dimer.

The DS distribution of the HPβCD dimer was also examined using a MALDI spectrum (Fig. S8). The spectrum exhibited a typical Gaussian-shaped distribution, indicating a composite isomeric mixture. The peak values corresponded to the sodium adduct of the selected DS. For instance, the value 2412.374/DS0 represented the molecular weight of the βCD dimer core plus one sodium unit, while the value 2470.590/DS1 represented the molecular weight of the βCD dimer core bearing one 2-hydroxypropyl moiety (DS1) plus one sodium unit, and so on.

The purity of the HPβCD dimer was determined using High-Performance Liquid Chromatography with Charged Aerosol Detection (HPLC-CAD), and it was measured to be >96 % based on the area percentage (Fig. S9). Lastly, the pH of a 30 % (w/v) aqueous solution of the HPβCD dimer at 25 °C was measured to be 8.3.

Additional characterization data and NMR spectra can be found in the supplemental information.

7KC was sourced from Cayman Chemicals (Ann Arbor, MI, USA), catalog number 16339, with a molecular weight of 400.6. Cholesterol was sourced from Sigma-Aldrich (St. Louis, MO, USA), catalog number C8667-5G, with a molecular weight of 386.65. Randomly Methylated βCD Monomers (RAMEB) were sourced from CycloLab (Budapest, HU). The molecular formula for RAMEB is $C_{42}H_{70-n}O_{35}\cdot(CH3)n$, the catalog number is CY-2004.1, and the CAS is CAS 128446-36-6. RAMEB has a molecular weight of 1135.0 + n·(14.0) and >95 % purity. The HPβCD monomer used in CiDi techniques was also sourced from CycloLab (Budapest, HU), catalog number CYL-4584, 96 % purity. Ethanol (EtOH) absolute was sourced from HiPerSolv Chromanorm, purity >99.7 %.

3. Methods

3.1. Computational methods

Computational methods are widely employed for characterizing protein-ligand interactions in both academic research and practical applications, including drug development. For such systems, numerous automated tools have been developed to facilitate the construction of structures and interaction parameters, generate and analyze quantitative trajectories, and visualize results. Nevertheless, CDs remain underexplored from a computational perspective, with most published results focusing on CD monomers. In this study, we have developed novel approaches to simulate and characterize CD dimer inclusion complexes, which have profound potential medical applications (Anderson et al., 2021).

3.1.1. Description of the structures employed for the computational simulations

One of the challenges in studying modified CDs, both computationally and experimentally, is that they are often not synthesized as a single isomer, but as a distribution of multiple molecular entities with different numbers and locations of substitutions and thus represented by an average DS. In contrast to *in vitro* experiments, it is feasible to consider a

limited number of individual chemical species from a computational perspective. Therefore, in this work, we will examine four distinct structures of HPβCD dimers (Fig. 2) which are expected to be present in the synthesized isomeric mixture, based on the selected synthetic conditions and on steric considerations, and as strongly suggested by the 1D and 2D in-depth NMR analysis (Figs. S1–7), to represent the distribution. To simulate the entire distribution of thousands of isomers in an isomeric mixture is, up to now, an elusive goal due to the calculation power required, so the discussion of the computational results will be limited to these reduced number of structures that will be taken as representative of the whole distribution.

The four structures have an asymmetric linker with 1 or 3 carbon atoms between the triazole ring and the first and second monomer, respectively. Although the 4 structures share the same linker, the number and location of the HP substituents are different. The first structure has only 2 substitutions at the interface between the two monomers and no substitutions within two GPU units of the linker. The second structure has four substitutions at the interface between the two monomers, and the last structure has all five substitutions located at the wide face of the monomers that face each other. Notably, S2 in structures 3 and 4 are identical.

CHOL and 7KC were employed as ligands to be encapsulated by the CD dimers. Unlike CDs, the chemical structures of these sterol molecules are well-defined (see Fig. 3). Our primary objective is to develop methods to selectively encapsulate 7KC without affecting CHOL concentration, as disrupting CHOL balance could have detrimental effects.

3.1.2. Simulation parameters

Both the initial coordinates for the CD dimers and the corresponding topologies were built using our own tools (Anderson et al., 2021). Initial coordinates and topology files for the sterol molecules were obtained from the ATB server (Malde et al., 2011). To ensure consistency with the force field, manual adjustments were made to the parameters, preventing unreasonable interaction constants for bonds and angles. Furthermore, the common atomic groups were assigned identical interaction parameters, while differences in interaction parameters were limited to the parts of the molecules that are not equivalent. After inserting the solute molecules (CHOL/7KC and CD) in a $10 \times 10 \times 10$ nm^3 dodecahedral simulation box, it was filled with approximately 23,000 SPC (simple point charge) waters (Berendsen et al., 1981), removing those overlapping the solute molecules. The NPT ensemble (constant-temperature, constant-pressure) at 298 K and 1 bar was employed in all cases. The temperature and pressure were controlled using the V-rescale thermostat (Bussi et al., 2007) and the Parrinello-Rahman barostat (Parrinello & Rahman, 1981) with coupling times of 0.1 and 0.5 ps, respectively. The long-range interactions were determined using the PME (Particle Mesh Ewald) (Darden et al., 1993; Essmann et al., 1995) algorithm with a grid spacing of 0.15 nm and a direct-space cut-off of 1.2 nm. The same cut-off was employed for the short-range interactions. A timestep of 2 fs was employed in all cases using the leap-frog integrator algorithm (Van Gunsteren & Berendsen, 1988). All bonds were constrained using the SETTLE algorithm (Miyamoto & Kollman, 1992) for water and the LINCS (Hess et al., 1997) algorithm for the CDs and the CHOL or 7KC molecules.

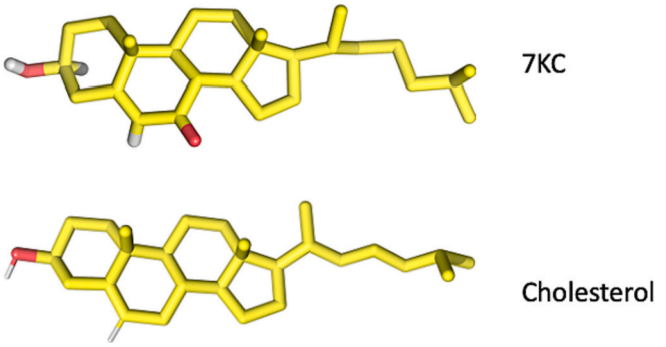

Fig. 3. Representation of the two sterol molecules, 7KC (top) and CHOL (bottom), considered. Carbon atoms are in yellow, polar hydrogens in white, and oxygen atoms in red. (For interpretation of the references to colour in this figure legend, the reader is referred to the web version of this article.)

In order to get the free energy profile leading to the formation of the complexes, as well as the optimal structure of the inclusion complex, well-tempered metadynamics simulations were performed. The most critical aspect of conducting these simulations involves the selection of a set of collective variables (CVs) able to effectively represent a pathway connecting the two states of the system. CD dimers possess numerous degrees of freedom, resulting in significant flexibility, which complicates the identification of a small set of generalized coordinates able to represent their dynamic behavior in a proper way.

The movement of CD dimers was constrained to focus on the characterization of double inclusion complexes (DIC, where "double" refers to both of the CD rings in the complex encapsulating the guest, as opposed to a "single inclusion complex" in which the stoichiometry is the same, but only one of the two CD rings encapsulates the guest), thus reducing the number of degrees of freedom and facilitating sampling. Although other structures may exist, such as various orientations of

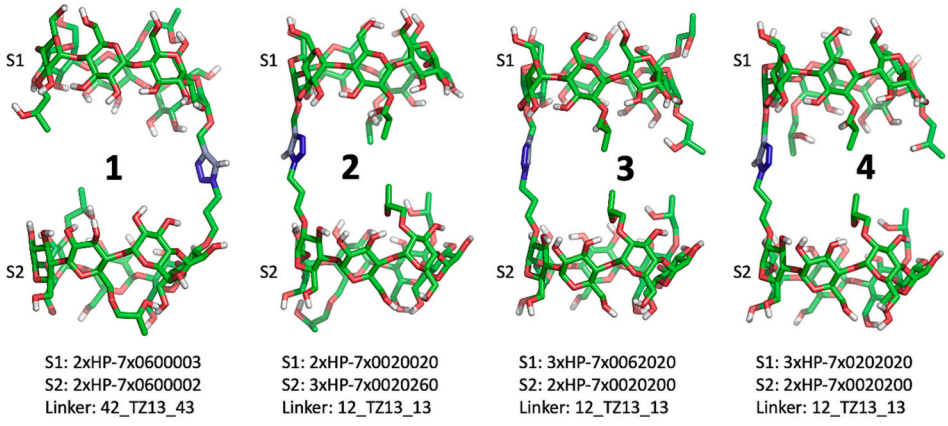

Fig. 2. Representation of the four CD dimers considered in our computational simulations. The sequence of each monomer subunit (S1 on top and S2 beneath) is indicated in the labels with the number of HP substitutions per monomer followed by the sequence of native or substituted glucopyranoside (GPU) units in the anticlockwise direction: 0 indicates no substitution (excluding the linker) in the corresponding GPU residue, while 2, 3 and 6 indicate the positions of the hydroxyl groups of the corresponding GPU residues. The location of the connection of the chemical linker to each CD monomer is also indicated with two digits per subunit as a prefix and a suffix to the acronym of the linker: 42_TZ13_43 indicates that the TZ13 linker is connected to the glucopyranoside number 4 of S1 at position 2 and to the glucopyranoside number 4 of S2 at position 3. The standard coloring of atoms is used, where carbon is green, oxygen is red, hydrogens are white, and nitrogen is blue. The number between both subunits in bold will be used to identify the structures along the text. (For interpretation of the references to colour in this figure legend, the reader is referred to the web version of this article.)

single inclusion complexes described in previous studies by free MD simulations (Anderson et al., 2021), it is anticipated that the major contribution to the binding constant will arise from the DIC configuration because the dimer was designed to form these types of extremely stable complexes. Thus, the following restraints were devised to focus the investigation on DIC structures: maintaining both CD monomers parallel to each other without angular or lateral shifts between their symmetry axes, permitting the ligand movement solely along the axis perpendicular to the plane of the CD monomers (identical for both subunits), and constraining the relative orientation of the ligand to approximately 0 or 180 degrees ("up" and "down" orientations, respectively) with the same axis. The "up" orientation corresponds to the complex with the tail of the sterol molecule pointing to the CD monomer joined to the shorter arm of the linker while the "down" orientation corresponds to the opposite orientation of the ligand in the CD dimer. Simulations with the "up" and "down" relative orientations of the ligand within the CD dimer were conducted separately. All restraints were implemented using harmonic potentials with a constant force of 1000 kJ·mol·nm.

For the CVs, we decided to use the distance between the center of mass (COM) of the ligand and the COM of the O4 atoms (those joining the glucopyranoside rings in the CD molecules) of each monomer as CVs (Fig. 4). The O4 atoms of each monomer were selected as reference points for distance measurements and defining reference planes and axes in the restraints, due to their relatively static nature compared to the other atoms within each CD monomer. These CVs allow for changes in the distance between both monomers and also the individual monomer-ligand distances, within range of the constraints.

Twelve coupled walkers starting from slightly different relative distances between each CD monomer and the ligand were used in parallel to execute the metadynamics simulations of each system and for each relative orientation of the ligand with respect to the CD dimer. These simulations were executed employing the GROMACS (Abraham et al., 2015; Berendsen et al., 1995) engine using the GROMOS53a6 forcefield (Oostenbrink et al., 2004) and PLUMED (Bonomi et al., 2009, 2019; Tribello et al., 2014) 2.8 with a reference gaussian height of 0.01 kJ/mol, a σ value of 0.1 nm, and a biasfactor parameter of 12. All the simulations were conducted for a minimum of 300 ns per walker.

3.1.3. Analysis

The PMF profiles were determined from the sum of the gaussian functions generated by the 12 walkers corresponding to each relative orientation of the CHOL or 7KC molecule with each CD dimer during the metadynamics trajectories, using the *sum_hills* tool of PLUMED. The one-dimensional projections of these profiles along each CV can be obtained by performing the numerical integration of the probability distribution associated with the two-dimensional PMF with respect to the complementary CV, also using the same tool. Subsequently, the resulting integrated values are transformed back into a PMF by taking the logarithm of these values, and then multiplying by the negative Boltzmann factor. The convergence of each simulation was also considered by plotting the evolution of the 1D-PMF profiles in time periods of 1 ns. The dispersion of these curves over the last 20 ns can be considered as a fingerprint of the convergence. The resulting 1D-PMF profiles were post-processed to determine the corresponding standard binding constant, which for a bimolecular interaction (A + B ↔ AB) can be determined from the partition function of each chemical species:

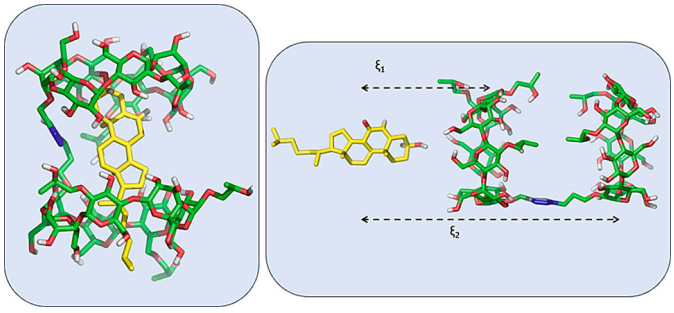

Fig. 4. Structure of a DIC comprising a HPβCD dimer with CHOL (left) together with the image of the separated sterol and CD dimer molecules illustrating the CVs (1 and 2) used for metadynamics simulations: the distances between the COM of the ligand and the COM of the O4 atoms of each CD monomer in the dimer. The colors and representation of the molecules are the same as in Figs. 2 and 3.

$$K_A = N_A \frac{Z_{AB} V}{Z_A Z_B} \tag{1}$$

where N_A is the Avogadro's number, Z_i is the partition function of the compound i and V is the volume of the system. Neglecting the internal degrees of freedom of A and B, the corresponding Hamiltonian is:

$$H_i = \sum_{j=1}^{3} \frac{p_j^2}{2m_i} \tag{2}$$

where p_j is the j component of the linear momentum and m_i is the mass of the molecule i. The partition function corresponding to that Hamiltonian is:

$$Z_i = V\left(\frac{2\pi m_i K_B T}{h^2}\right)^{3/2} \tag{3}$$

with K_B representing the Boltzmann constant and h the Plank constant. The Hamiltonian corresponding to the complex would be:

$$H_{AB} = \sum_{j=1}^{3} \frac{\left(p_j^{com}\right)^2}{2(m_A + m_B)} + \sum_{j=1}^{3} \frac{\left(p_j^{R}\right)^2}{2\mu} + E(r) \tag{4}$$

p_j^{com} being the j component of the linear momentum of the COM of the complex, p_j^R the j component of the linear momentum of the relative movement between A and B in the complex, $\mu = m_A \cdot m_B / (m_A + m_B)$, and E(r) is the potential energy of interaction between A and B (the PMF) as a function of the relative coordinates between both molecules (r). The corresponding partition function is:

$$Z_{AB} = V\left(\frac{2\pi(m_A + m_B)K_B T}{h^2}\right)^{3/2}\left(\frac{2\pi\mu K_B T}{h^2}\right)^{3/2}\int e^{-E(r)/RT} dr \tag{5}$$

where R and T are the gas constant and the temperature, respectively. Replacing Eqs. (3) and (5) in Eq. (1), we get the following equation (Piñeiro et al., 2022):

$$K_A = N_A \int e^{-E(r)/RT} dr \tag{6}$$

Given the restraints applied to the internal flexibility of the CD dimer and to the relative movement and orientation of the sterol molecule with respect to the macromolecule, the interaction energy E(r) and the volume element dr can be expressed in terms of cylindrical coordinates (ϕ, ρ, z). Since the rotations around the principal axis are not restrained, and the PMF is assumed to be independent on the corresponding angle, the volume element can be integrated over ϕ (from 0 to 2π). The distance from the ligand to the axis perpendicular to the O4 atoms that passes throughout the COM of these atoms is restrained with a harmonic potential, so it is not exactly constant, but the PMF is assumed to be independent on this parameter. Thus, the volume element is also integrated over r from 0 to r_{max}, which is assumed to be 3 Å in all cases (as an approach to the radius of the CD). Finally, the 1D projection of the PMF is a function just on each x_i, and the binding constant can be determined by:

$$K_A = \pi N_A \rho_{max}^2 \int e^{-E(\xi_i)/RT} d\xi_i \tag{7}$$

The binding constant for each system was computed by numerical integration of the two possible projections of the PMF along each CV. In order to estimate the uncertainty of the K_A values, multiple integrations were considered for each 1D-PMF, with different integration limits in the unbound region. All the resulting values were then clusterized and the final K_A value with its uncertainty was calculated from the average value and the standard deviation of the mean considering only the values of the most populated cluster. This approach resulted in a fully automated 2D PMF method, providing a reasonable quantitative approach for obtaining binding constants for the formation of 1:1-DICs using a reasonable amount of computational resources. The final values of K_A and the corresponding ΔG^0 were obtained using a Python script that uses the pandas (McKinney, 2010; team, 2023), numPy (Harris et al., 2020), matplotlib (Hunter, 2007), and kmeans1d (Grønlund et al., 2018; Wu, 1991) libraries.

3.2. In vitro methods

3.2.1. Isothermal titration calorimetry

ITC experiments are widely recognized as the gold standard for characterizing the thermodynamics of molecular interactions. This is because they rely on a direct measurement of the interaction energy as a function of time (heat power), which, when integrated, yields the enthalpy as a function of the concentration ratio of the involved compounds. The analysis of the corresponding isotherms offers insights on the interaction mechanism (stoichiometry), as well as the corresponding binding constants for the applied model. Additionally, no chemical labeling is required to perform the experiments, but they do require that the compounds are well-dissolved at concentrations that yield significant signals. The low solubility of the studied solute, in this case sterol molecules, is a common limitation in such studies, since their solubility is lower than that required to get a clear signal in the calorimeter. Thus, we designed an alternative strategy to characterize interactions with CD dimers, using randomly methylated βCD monomers (RAMEB) as a competitor to encapsulate sterol molecules. This is similar to the "release protocol" found effective for analysis of CD monomers, in which a saturated solution of Target 1 encapsulated CD is titrated with a second target solution capable of displacing the Target 1 from the CD (Bertaut & Landy, 2014; Bouchemal & Mazzaferro, 2012). For our assay, 40 small (12 μL) aliquots of approximately 10–20 mM RAMEB and around 1 mM sterol solutions were injected into the sample cell of a VPT-ITC from Microcal containing either pure water (for dilution experiments) or CD dimer aqueous solutions at about 0.04–0.08 mM (for competitive experiments). The employed RAMEB to sterol concentration ratio (10–20:1) was required to fully solubilize the sterol molecule. The sample cell and the syringe were carefully cleaned with DMSO and water between experiments.

The ITC raw data were processed (baseline correction + integration of the power profile) using the AFFINImeter software (Piñeiro et al., 2019), since it allows a flexible definition of several coupled equilibrium processes to be simultaneously considered as a global interaction model. The results were then fitted with a competitive model where the sterol (S) can be encapsulated either in the monomer (M) or in the dimer (D) with different stoichiometries represented by the following equilibria:

$$M + S \rightleftharpoons M_1S_1 \Rightarrow K = \frac{[M_1S_1]}{[M][S]} \tag{8}$$

$$2M + S \rightleftharpoons M_2S_1 \Rightarrow K = \frac{[M_2S_1]}{[M]^2[S]} \tag{9}$$

$$D + S \rightleftharpoons D_1S_1 \Rightarrow K = \frac{[D_1S_1]}{[D][S]} \tag{10}$$

$$D + 2S \rightleftharpoons D_1S_2 \Rightarrow K = \frac{[D_1S_2]}{[D][S]^2} \tag{11}$$

$$2D + S \rightleftharpoons D_2S_1 \Rightarrow K = \frac{[D_2S_1]}{[D]^2[S]} \tag{12}$$

3.2.2. Electronic spectroscopy

UV–Vis Absorption spectra have been registered on a Perkin Elmer 950 spectrophotometer. The intrinsic absorption of the triazole linker in the dimer was used with a molar absorption coefficient of 4000 M^{-1} cm^{-1} at 215 nm to estimate the CD concentration. CiDi spectra have been registered on a Jasco J-715 spectropolarimeter. The CiDi experiments were performed in diluted aqueous solutions of the sterol with a minimal amount of EtOH (1 % V/V) in order to avoid aggregation phenomena or precipitation, and to circumvent the use of the intrinsic aqueous solubility value of the sterol during the estimation of the binding constants. The 7KC or CHOL concentration in the aqueous solution has been set to 20 μM, close to its solubility limit in water (6 μM) allowing the recording of reliable CiDi spectra, with the CD concentration varying in the 20–200 μM range. The CiDi spectra of the sterol/CD mixtures were corrected for the CiDi signal of the quartz cuvette with solvent. The best complexation model, binding constants, and single spectra of the complexes were determined by means of a multivariate global analysis of multiwavelength data using a set of spectra corresponding to different sterol/CD mixtures. The analysis was performed with the commercial software ReactLab™ Equilibria from JPlus Consulting developed by Matlab (MathWorks—Makers of MATLAB and Simulink, n.d.), considering the equilibrium processes in Eqs. (10)–(12). The ReactLab™ Equilibria procedure is based on singular value decomposition (SVD) and nonlinear regression modeling by the Levenberg-Marquardt method. A matrix is created with all complete absorption or CiDi spectra, and each spectrum is assigned to a specific CD concentration of the titration. The analysis proceeds by optimizing the single binding constants as well as the spectra of the single species. It eventually affords, upon convergence, the final binding constants of the chosen model together with the individual spectra of the complexes. The software allows comparison of experimental data and calculated values at single wavelengths to evaluate goodness of fit. Further statistical outputs include standard deviations for each fitted parameter as well as sum-of-squares and standard deviation for the residuals.

4. Results

4.1. Metadynamics simulations

Two-dimensional PMF profiles, the structures of the optimized supramolecular complexes with 1:1 stoichiometry, and an estimation of the corresponding binding constants were obtained from metadynamics simulations (Fig. 5 and Table 1). The structures of the four dimers are shown in Fig. 2.

The analysis obtained from metadynamics simulations provides a significant amount of energetic and structural information showing clear trends. It is worth keeping in mind that the two relative orientations of the sterol molecule in the cavity of the CD dimer are not equivalent, as the linker is asymmetrical, which explains the different results for both orientations of the ligand. For CD dimer 1, which has the fewest number of HP substituents at the interface, the minimum energy structures for the "down" orientation are tightly packed for both sterol molecules, with the COM of the ligand at only 0.106 nm of S1 for CHOL and 0.105 nm of the same subunit for 7KC, while the distances to S2 are 0.706 and 0.671, respectively. Although the structures appear similar, the energy well for 7KC is much deeper, resulting in a considerably larger binding constant. This is a clear indication of specificity, as the same CD dimer can effectively distinguish between the two sterol molecules. Note that the "down" orientation corresponds to the complex with the tail of the sterol molecule pointing towards the CD monomer connected to the longer arm of the linker. In contrast, the structures corresponding to the "up" orientation are less compact, with the

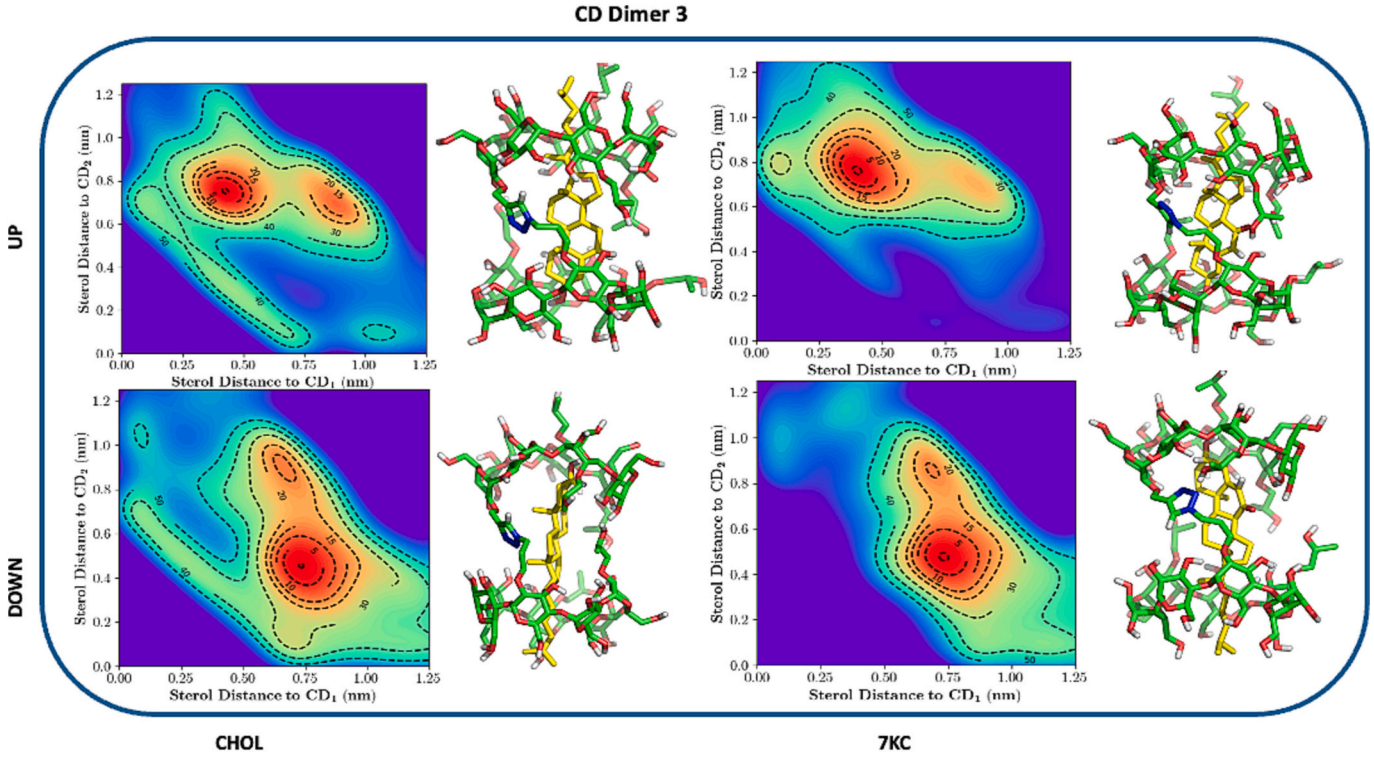

Fig. 5. PMF profiles obtained from metadynamics simulations together with the minimum energy structure for each case. Results for each CD dimer structure are separated and labeled. The upper row of each panel presents the "up" relative orientation of the ligand within the CD cavity, while the bottom row shows the "down" orientation. CHOL results are displayed on the left side, and 7KC results are on the right side of each panel. The full PMF results are supplemented in Fig. S10.

Table 1
Binding constants in M^{-1} for the different CD dimers and sterol molecules used in the metadynamics simulations, obtained from the sum of K_{av} shown in Table S1. The uncertainties are given in percentages.

CD dimer:	1	2	3	4
CHOL	$2.66 \cdot 10^5 \pm$ 17 %	$2.00 \cdot 10^7 \pm$ 5.6 %	$2.12 \cdot 10^6 \pm$ 9.8 %	$5.97 \cdot 10^7 \pm$ 8.9 %
7KC	$4.25 \cdot 10^8 \pm$ 7.0 %	$3.16 \cdot 10^7 \pm$ 6.7 %	$2.56 \cdot 10^8 \pm$ 12 %	$2.49 \cdot 10^6 \pm$ 6.0 %

monomers more separated from each other, and the corresponding binding constants significantly lower than those for the "down" orientation.

In general, the PMF profiles for the same CD dimer and orientation are similar for both sterol molecules with surprisingly high reproducibility of the distances between the sterol and each of the CD subunits (Table S1). However, there are substantial quantitative differences in the energy values. The most similar energy profiles between the sterol molecules correspond to CD dimers 2 and 3. Notably, several PMF profiles, mainly those corresponding to the "up" orientation, contain two energy wells, suggesting that the same CD dimer could simultaneously bind two sterol molecules at different locations.

It can easily be demonstrated that the overall binding constant corresponding to a given complex, considering both possible orientations, can be obtained by adding the separate values obtained for each orientation. To facilitate a clearer comparison between the results obtained for the four structures and the two sterol molecules, the results are summarized in Table 1, considering just one binding constant per system.

These results clearly indicate that the structure **1**, with (1) the lowest number of substituents in the interface between both CD monomers, (2) the fewest number of substitutions close to the linker, and (3) the lowest number of substitutions overall, exhibits the highest specificity towards 7KC. Moreover, it is evident that, on average, these isomers of the HPβCD dimer prefer to encapsulate 7KC over CHOL. This is in agreement with previously published relative affinities estimated *in vitro* by turbidity assay and NMR (Anderson et al., 2021). Structure **2**, with the most substitutions on the CD bound to the short side of the linker, shows poor specificity for 7KC, indicating that the number and position of substitutions on each monomer in an asymmetrically linked dimer may contribute to specificity. Only the structure **4**, with both the highest number of substitutions at the interface and the highest number of substitutions closest to the linker, shows a preference for CHOL over 7KC, indicating that the substitutions at the CD-CD interface may contribute more to specificity than other factors. These results indicate that the number and location of the substitutions in each subunit relative to each other and the linker are important factors in inclusion complex formation, and may be the key to improving specificity for particular guest molecules.

4.2. *Competitive isothermal titration calorimetry*

Before studying the sterol-dimer interaction in competition experiments using ITC, dilution experiments were performed with the sterol-RAMEB mixtures. Interestingly, the energy profiles of the dilution experiments for the mixtures of RAMEB CD monomers with 7KC and CHOL are strikingly different (Fig. 6). This indicates that ITC clearly distinguishes the interaction between each sterol and the CD monomer, which is apparent by eye without the application of any theoretical model, despite the subtle difference between the structures of these two sterols (Fig. 3). For CHOL + RAMEB CD monomers, a global analysis of the different experiments, using multiple seeds for the numerical calculations as implemented in AFFINImeter, was performed (Piñeiro et al., 2019). A model that incorporates both 1:1 and 2:1 (CD_2:$CHOL_1$) complexes was required to fairly describe the experimental isotherms (Eqs. (8) and (9)). The binding constants resulting from this global fitting of

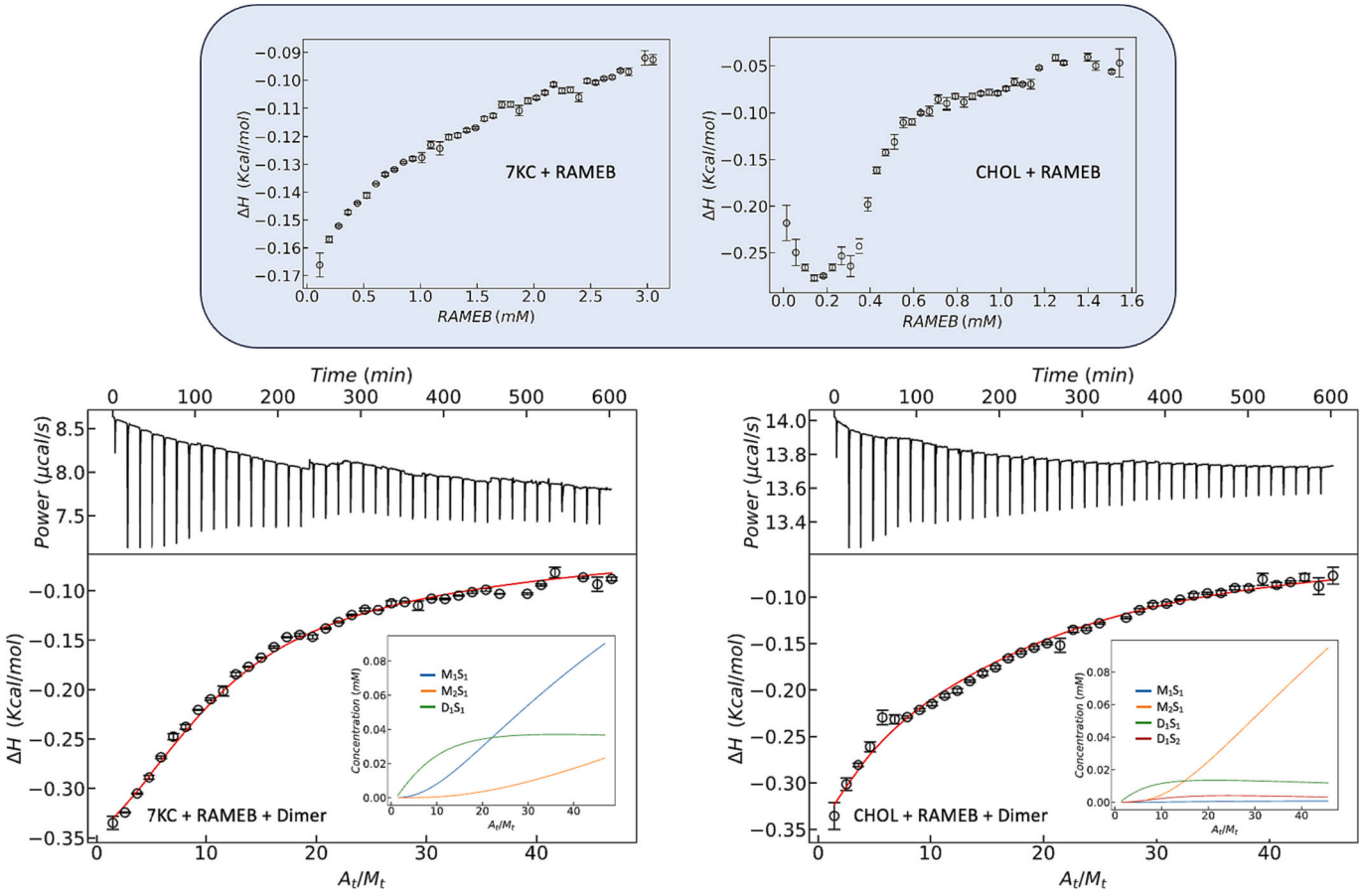

Fig. 6. ITC results corresponding to the ITC dilution experiments (top) of RAMEB + sterol and the global fitting of sterol + RAMEB + CD dimer (bottom) for 7KC (left) and CHOL (right). The dilution experiments (top) show that ITC clearly distinguishes the interaction between the sterol and the CD monomer, and that 7KC has a simpler and stronger interaction than CHOL. The competitive experiments (bottom) show much stronger binding between sterols and CD dimers than monomers. The insets show the concentration of M_1S_1 (blue line), M_2S_1 (orange line), D_1S_1 (green line), and D_1S_2 (red line). The concentrations employed for each experiment are indicated in the plots. The full ITC results are supplemented in Fig. S11. (For interpretation of the references to colour in this figure legend, the reader is referred to the web version of this article.)

the monomer data reveal that the formation of 1:1 complexes is unfavorable compared to 2:1 complexes. Despite its very low concentration in the explored conditions, the presence of the 1:1 complex is essential for an accurate depiction of the curvature changes for CHOL. For 7KC, the dilution experiments clearly show a different profile compared to that of CHOL (Fig. 6, top). Global analysis of the 7KC ITC data also required a model with two complexes of 1:1 and 2:1 stoichiometry, but with a much more favorable binding constant for 1:1 complexes.

The thermodynamic parameters corresponding to the interaction between CHOL and RAMEB were considered to analyze the competitive experiments including the CD dimer. Three independent replicates of these experiments at slightly different concentrations were performed and, again, they were globally analyzed. Fittings assuming that CHOL and the dimer form only a 1:1 complex were unable to successfully describe the experimental data, so it was necessary to consider the presence of an additional chemical species. After several tests, it was observed that the data can be reasonably well described considering also the presence of 1:2 complexes, where two CHOL molecules interact with a single dimer (Fig. S12), albeit with high uncertainties in the thermodynamic parameters. The possible encapsulation of two sterol molecules by a single CD dimer is consistent with the presence of two energy wells observed in some of the PMF profiles (*e.g.* that corresponding to the CD dimer 3 interacting with CHOL in the "up" relative orientation shown in Fig. 5), and this phenomenon has been observed in unrestrained simulations by our group (data not shown). The high uncertainties of the parameters could be attributed to the fact that both CDs are a distribution of multiple molecules with different locations and numbers of substituents, introducing additional uncertainty and complexity. Therefore, we propose that the thermodynamic parameters obtained from this analysis (Tables 2 and 3) are representative values for the entire CD distribution in the sample.

It is worth mentioning that both the 1:1 and the 1:2 complexes between the CD dimer and CHOL are present in the sample at significant concentrations, in contrast to what was observed for the interaction between RAMEB and this sterol molecule, which displays a clear cooperative behavior in favor of the 2:1 ($CD_2Sterol_1$) complexes. The binding constants corresponding to the formation of the 1:1 and 1:2 complexes, as described in Eqs. (10) and (11), cannot be compared as they correspond to reactions of different degrees, thus resulting in different units. However, it is possible to compare the K-value of Eq. (10) with the *ratio* between the K-values of Eqs. (11) and (10), which represents the formation of the 1:2 complexes from the addition of a second sterol

Table 2
Binding constants and enthalpies for the equilibria indicated in the first column, where M stands for RAMEB, D for the CD dimer, and S for the sterol, obtained from the analysis of dilution and competitive ITC experiments.

S = CHOL	K (M^{-n})	ΔH (kcal/mol)
$M + S \leftrightarrow M_1S_1$	$58.2 \pm 3.0\ M^{-1}$	-121 ± 54
$2\,M + S \leftrightarrow M_2S_1$	$(5.631 \pm 0.050) \times 10^6\ M^{-2}$	2.2345 ± 0.008
$D + S \leftrightarrow D_1S_1$	$(6.5 \pm 20) \times 10^4\ M^{-1}$	-1.59 ± 0.11
$D + 2S \leftrightarrow D_1S_2$	$(1.79 \pm 0.36) \times 10^9\ M^{-2}$	7.3 ± 4.3

Table 3
Binding constants and enthalpies for the equilibria indicated in the first column, for 7KC, obtained from the global analysis of dilution and competitive ITC experiments.

S = 7KC	K (M^{-n})	ΔH (kcal/mol)
$M + S \leftrightarrow M_1S_1$	$(5.01 \pm 0.35) \times 10^4\ M^{-1}$	5.18 ± 0.42
$2\ M + S \leftrightarrow M_2S_1$	$(4.49 \pm 0.34) \times 10^6\ M^{-2}$	8.09 ± 0.42
$D + S \leftrightarrow D_1S_1$	$(2.02 \pm 0.15) \times 10^7\ M^{-1}$	0.99 ± 0.43
$D + 2S \leftrightarrow D_1S_2$	N/A	N/A

molecule to the already formed 1:1 complex. This latter value, approximating the overall affinity between the steroid and the CD, is $(1.79 \times 10^9) / (6.5 \times 10^4) = 2.75 \times 10^4\ M^{-1}$. This is slightly lower than the K-value corresponding to the formation of the 1:1 complexes from the free molecules.

$$K_{stepwise} = \frac{[D_1S_2]}{[D_1S_1][S]} \quad (13)$$

For 7KC, the competitive experiments involving the CD dimer were satisfactorily described considering just a 1:1 complex between 7KC and the dimer, with a binding constant of $\sim 2.0 \cdot 10^7\ M^{-1}$ (Table 3). This binding constant is similar to the values determined from metadynamics simulations, although a direct comparison should not be made because the ITC experiments consider all the chemical species collectively while the computational calculations distinguish structures with specific numbers and locations of the HP substituents. In contrast to what was observed for the interaction with CHOL, the enthalpies corresponding to 7KC were found to be positive in all cases. This explains the qualitatively different behavior between both sterols observed in Fig. 6.

Overall, it can be concluded that ITC is able to effectively differentiate between the two sterol molecules, despite differing by only 1 atom, not only from the quantitative point of view but also by identifying different interaction schemes. Importantly, it was also found that the affinity of the dimer for 7KC is significantly higher than that for CHOL.

4.3. Circular dichroism

Fig. 7A and E show the CiDi spectra obtained by titrating CHOL or 7KC with increasing dimer concentrations. Tables 4 and 5 report the binding constants for the equilibria in Eqs. (10) and (12) obtained with the CiDi technique.

In the case of CHOL, it was possible to monitor the intrinsic sterol CiDi signal at 205 nm becoming less intense with increasing CD dimer concentration (Fig. 7). The absorption spectra are dominated by the dimer triazole absorbance (Fig. S14). Differently from 7KC, analysis does not converge when applying a model with the simultaneous presence of two complexes with different stoichiometries. The CiDi and absorption data (Table S3, Fig. S14) both converged when fitted to a model with only one complex with 1:1 stoichiometry, and the binding constants were similar between the two methods. Table 4 reports the binding constant obtained with CiDi. The result of the fitting with the 1:1 model is in good agreement with the ITC results.

Table 4
Binding constants for the equilibria indicated in the first column for CHOL, obtained from the global analysis of CiDi experiments, converging with the model in the presence of a single complex for CHOL.

S = CHOL	K (M^{-n})
$D + S \leftrightarrow D_1S_1$	$(3.8 \pm 0.2) \times 10^4\ M^{-1}$

Table 5
Binding constants for the equilibria indicated in the first column, for 7KC, obtained from the global analysis of CiDi experiments, converging with the model in presence of two complexes for 7KC.

S = 7KC	K (M^{-n})
$D + S \leftrightarrow D_1S_1$	$(7.05 \pm 2.20) \times 10^7\ M^{-1}$
$2D + S \leftrightarrow D_2S_1$	$(1.51 \pm 0.48) \times 10^{13}\ M^{-2}$

Regarding 7KC, analysis of CiDi data required a model with two complexes with different stoichiometries when analyzing the entire range from 200 to 400 nm. The analysis does not converge when fitting with a model of only one complex with 1:1 or 2:1 (dimer:7KC) stoichiometry. This is not surprising, considering the ellipticity plots at selected wavelengths shown in Fig. 7F. In particular, for the negative band in the 216 nm region of 7KC, there is an ellipticity trend that inverts halfway through titration, different from the positive band in the 300–350 nm region, due to the C═O functionality where there is a small decrease and shift in maximum (Marconi et al., 2011). Analysis of the 7KC absorption spectra confirmed the model with 2 complexes of different stoichiometry, but yielded binding constant values that were lower (Figs. S13, S14), perhaps because CiDi can more easily sense when changes occur in complex stoichiometry and geometry compared to the absorption

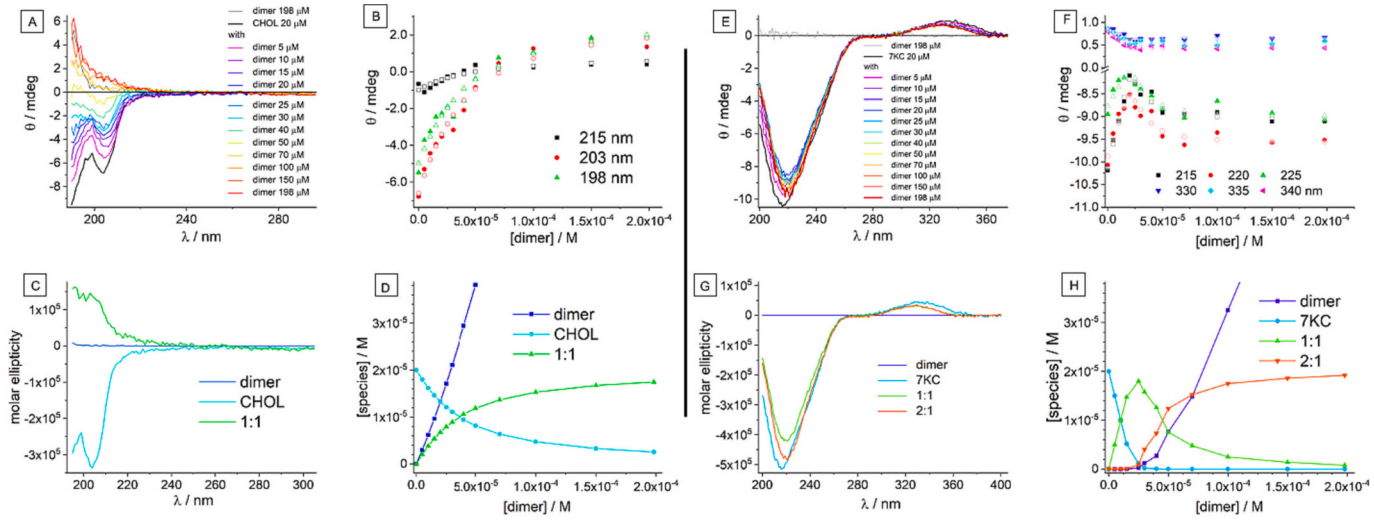

Fig. 7. Original CiDi spectra of 20 μM solutions of CHOL (left, A) and 7KC (E) with increasing dimer concentrations (5–200 μM) in a 1 cm cuvette; (B, F) plots of absolute (full symbols) and calculated ellipticity values (empty symbols) at selected wavelengths (nm) for CHOL (B) and 7KC (F); (C, G) calculated spectra of the free components and complexes of the best models for CHOL (C) and 7KC (G); (D, H) species distribution *vs* total dimer concentration for CHOL (D) and 7KC (H).

technique. Indeed, the CiDi spectrum of the dimer is almost flat in the 200–400 nm range, and the CiDi signal is therefore due to 7KC (with a very intense intrinsic signal). Complexation and interaction with the dimer triazole unit may give rise to an induced signal in the complex, but the shape of the collected CiDi spectra along titration suggests the origin of the observed signal is mainly due to the 7KC unit in the complex. Moreover, the UV changes are very small for 7KC and no relevant trend inversion was observed at any wavelength.

As for the spectral characteristics for the 7KC complexes, the positive band at 350 nm is typical of the C═O bond and the more intense negative band at 220 nm is typical of the conjugated system C═C—C═O, due to n-π* and π-π* transitions, respectively. It is likely that they are both strongly influenced in the 1:1 complex, where we can envision a rigid geometry. A more flexible geometry in the 2:1 complex may allow the π-π* transition to recover in intensity. The lone electron pair of the carbonyl oxygen may be involved in hydrogen bonding in both complexes, thus explaining why its signal does not change when going from 1:1 to 2:1 stoichiometry.

An additional study has been conducted using CiDi to characterize the interaction of 7KC and CHOL with the HPβCD monomer. In this case, a single trend of decreasing ellipticity was observed around 220 nm and in the 300–350 nm range for 7KC and 205 nm for CHOL (Figs. S15, S16). Analysis converged with the exclusive presence of a 2:1 complex of 2 CD monomers for one steroid molecule (Table S4). The overall binding constants of the 2:1 complexes of 7KC and CHOL with the monomer were much lower compared to the dimer. A similar preference of HPβCD monomers for 7KC over cholesterol was also observed.

The results ultimately show that the CD dimer has a very high affinity for 7KC. Furthermore, the CD dimer has a higher affinity for 7KC than it does for CHOL. Monomeric HPβCD has a much lower affinity for both CHOL and 7KC. The dimer binding constants are in line with values reported in the literature for other CD dimers complexing CHOL (Alcalde et al., 2009; Breslow & Zhang, 1996; Kritharides et al., 1996; Nishijo et al., 2003).

5. Discussion

This study forms part of a broader project aimed at designing modified CDs capable of encapsulating toxic biomolecules with high affinity and specificity. This project aims to quantify this interaction by obtaining binding constants for the CD dimer - sterol inclusion complex, but is applicable to any CD dimer inclusion complex. Numerous methods may be employed to perform this characterization, but none of them represent a universal solution for every system. In the case of the interaction between CD dimers and sterol molecules, several difficulties are evident: first, modified CDs are often constituted by a mixture of numerous species with varying number and location of modified groups; second, the sterols targeted in this study are highly insoluble in aqueous media; finally, there are multiple stoichiometries at play, and accounting for all of them is challenging. Here we have utilized one *in silico* and two *in vitro* techniques to synergistically address these problems; namely: PMF calculations from metadynamics simulations, as well as global analysis of multiple competitive ITC and CiDi measurements.

5.1. In Silico

The convergence of the metadynamics simulations using the distance between the COM of the ligand and of each monomer as collective variables was satisfactory at time scales of 300 ns using 12 walkers and a combination of restraints designed to bias the reversible formation of 1:1 DICs. Under these conditions, the obtained binding constants indicate that the presence of 2-hydroxypropyl substituents at the interface between both monomers in the CD dimer hinders the ability of the CD dimer to distinguish between the sterol molecules. Thus, the CD with a lower number of HP groups in that region shows the highest affinity for 7KC as well as the highest specificity to capture this sterol molecule. This is consistent with previously published work using less quantitative methods for comparing the complexes (Anderson et al., 2021). Previous unbiased molecular dynamics simulations suggested that CD dimers form more stable complexes with sterols than do monomers, and that there was some preference for complexing with 7KC over CHOL, however such calculations did not allow the quantitative characterization of the interactions. Previous crude turbidity tests showed that CD dimers could solubilize 50 % of 7KC at a ~10× lower concentration of CD than CHOL, but the difference in concentration does not reflect even the relative difference in actual affinity demonstrated in the present work, which was closer to 1000× using rigorous biophysical methods. It is worth noting that turbidity measurements can be affected by different molecular interaction mechanisms other than the simple formation of 1:1 inclusion complexes. NMR has also shown the same dimer encapsulating both 7KC and CHOL predominantly in 1:1 double-inclusion complexes, but the model proposed for the 7KC complex appeared to be more clear and consistent than that with CHOL (Anderson et al., 2021). The computational method employed in the present work is exceptional for studying specific modified CD molecules with a predetermined number and location of the substituted groups, but it cannot be directly employed to derive the apparent binding constant for a whole distribution formed by an astronomical number of different structures present in a non-isomeric mixture typical of randomly substituted CDs.

5.2. In Vitro

Both ITC and CiDi enable quantification while considering the overall contribution of the entire distribution of different molecular structures that are present in the sample, and distinguish between the different stoichiometries in the mixture, while the simulations currently focus on a single isomer at a time in the 1:1-DIC complex. CiDi has an advantage over ITC in that the technique does not require competition between two encapsulators for these systems, in this case the dimer and RAMEB. ITC, on the other hand, by virtue of the fact that it directly measures the heat (energy) difference between states, might be considered a more direct and empirical quantification of binding. Both *in vitro* methods indicate that the 1:1 complexes have the most favorable binding constant especially for 7KC, and to a lesser extent for CHOL. Further, both *in vitro* techniques reveal complexes with additional stoichiometries to be considered, and that those stoichiometric contributions are different between 7KC and CHOL (which is surprising, considering the molecules differ by only one atom, but also encouraging as we are seeking selectivity for 7KC over cholesterol (Anderson et al., 2021)). Importantly, the concentration ratio of CD to sterol is different between CiDi and ITC, which could impact the interpretation of the stoichiometry and/or binding constants. For example, the CiDi concentration range accounts for the 2:1 (CD:sterol) complex, while ITC accounts for the 1:2 (CD:sterol) complex, making the methods complementary in this respect, but the obtained binding constants broadly agree between the two *in vitro* methods. By most measures, 1:1 complexes dominate the interaction, while ITC suggests that there may be a significant presence of 1:2 complexes between the CD dimer and CHOL. Interestingly, ITC clearly shows that both sterol molecules can be distinguished by RAMEB CD monomers, even at the qualitative level and out of model considerations, which was a surprising result. Noticeably, in the case of 7KC, the interaction is always entropy-driven. A possible reason may be the more rigid skeleton of 7KC compared to CHOL (due to sp2 hybridization of the 7 carbon in 7KC compared to sp3 of the same carbon in CHOL), preventing 7KC from optimizing the non-covalent interactions with the CD. The interaction may thus be exclusively entropy-driven in the case of 7KC, and solvation effects are likely important. Another hypothesis, which supports entropy-driven processes, is the co-existence of more conformations for a single complex, as suggested by the calculations that find two energy wells in several cases. Finally, in the case of CHOL, the 1:1 complex with the dimer has a

favorable enthalpy, likely due to multiple optimized non-covalent interactions. In the complex with two sterols, solvation effects are expected to be more important, and also multiple conformations may exist.

The structure of CD inclusion complexes is pivotal in their ability to effectively distinguish between 7KC and CHOL, and therefore potentially mitigate 7KC toxicity in a biological setting. For the studied CD dimers, the 1:1 complex is the strongest, and computational studies indicate that this complex is likely a DIC (Fig. 5). This complex is more favorable for 7KC than for CHOL, despite the only subtle difference between the molecular structures of 7KC and CHOL. Noncovalent interactions stabilize the inclusion complex, so a slight difference in rigidity and/or hydrophobicity can convey a significant difference in the binding constant for CD inclusion complexes. Additionally, our previous publication details the impact of the substitutions and linker on the strength and specificity of the interaction compared to other dimers. In this previous study, a small number of HP groups in combination with the triazole group on the linker exhibited the best 7KC specificity at a qualitative level (possibly caused by a destabilizing effect on the cholesterol inclusion complex) (Anderson et al., 2021). The present study supports that hypothesis, and elucidates quantitative binding constants for this one dimer.

6. Conclusion

The combined results of these experiments demonstrate that the CD dimer has ~1000 fold stronger affinity for 7KC than for CHOL. The binding constants obtained from the *in vitro* methods compare well with those obtained from metadynamics simulations, and they are comparable or even higher than other values reported in literature for similar systems of steroid complexes with CD dimers (Christoforides et al., 2018; Kritharides et al., 1996; Piñeiro et al., 2007). While some of the inclusion complex properties remain difficult to characterize, the combined methods demonstrate the ability of CD dimers to quantitatively differentiate between very similar guest molecules.

This work underscores the challenges of obtaining realistic binding constants for complex systems, as well as the advantages and disadvantages of three different methods. Here, specific protocols have been developed to optimize the characterization of these systems by conducting an orthogonal study based on three different methods to obtain complementary information. In particular, the power of iterating between multiple simulations of single isomers and empirical *in vitro* data from non-isomeric mixtures of host molecules should not be underappreciated. While computational data always needs to be validated with physical data, simulations allow for predictions, enriched interpretation of empirical experiments, and the isolation of questions that cannot be asked in real-world experiments. The combination of the two helps explain the true nature of the complex better than either on its own. This study is expected to serve as a benchmark in the characterization of other, similarly complex systems. The remarkable capability of these CD dimers to discriminate between targets as similar as CHOL and 7KC, both qualitatively and quantitatively, highlights the potential for leveraging CDs in the specific encapsulation of particular small molecules for diverse applications.

CRediT authorship contribution statement

Amelia M. Anderson: Conceptualization, Methodology, Software, Validation, Formal analysis, Investigation, Writing – original draft, Writing – review & editing, Visualization, Project administration. **Ilse Manet:** Methodology, Validation, Formal analysis, Investigation, Resources, Writing – original draft, Writing – review & editing, Visualization. **Milo Malanga:** Validation, Methodology, Resources, Writing – review & editing, Project administration. **Daniel M. Clemens:** Conceptualization, Writing – review & editing. **Keivan Sadrerafi:** Conceptualization, Writing – review & editing, Methodology, Resources, Supervision. **Ángel Piñeiro:** Conceptualization, Methodology, Software, Validation, Formal analysis, Investigation, Resources, Writing – original draft, Writing – review & editing, Visualization, Supervision. **Rebeca García-Fandiño:** Conceptualization, Methodology, Software, Validation, Formal analysis, Investigation, Resources, Writing – original draft, Writing – review & editing, Visualization, Supervision. **Matthew S. O'Connor:** Conceptualization, Writing – original draft, Writing – review & editing, Supervision, Project administration, Funding acquisition.

Declaration of generative AI and AI-assisted technologies in the writing process

During the preparation of this work the author(s) used OpenAI's ChatGPT in order to improve the readability and flow of the manuscript. After using this tool/service, the author(s) reviewed and edited the content as needed and take full responsibility for the content of the publication.

Declaration of competing interest

The authors declare the following financial interests/personal relationships which may be considered as potential competing interests: All authors report financial support, administrative support, equipment, drugs, or supplies, travel, and writing assistance were provided by Cyclarity Therapeutics. Amelia Anderson and Matthew O'Connor have patent Cyclodextrin dimers, compositions thereof, and uses thereof pending to CYCLARITY THERAPUTICS, INC.

The authors would like to disclose that AMA, KS, DMC, and MSO have a financial interest in the company Cyclarity Therapeutics. MM has a financial interest in the company CarboHyde; RGF and AP have a financial interest in the company MD.USE. Cyclarity Therapeutics commissioned this work from all authors.

Data availability

The data that has been used is confidential.

Acknowledgements

This work was supported by funding from Cyclarity Therapeutics. The authors would also like to thank CESGA (Galicia Supercomputing Center) for their collaboration and expertise in optimizing computing time and services.

References

Abraham, M. J., Murtola, T., Schulz, R., Páll, S., Smith, J. C., Hess, B., & Lindahl, E. (2015). GROMACS: High performance molecular simulations through multi-level parallelism from laptops to supercomputers. *SoftwareX, 1–2*, 19–25. https://doi.org/10.1016/j.softx.2015.06.001

Aime, S., Gianolio, E., Arena, F., Barge, A., Martina, K., Heropoulos, G., & Cravotto, G. (2009). New cyclodextrin dimers and trimers capable of forming supramolecular adducts with shape-specific ligands. *Organic & Biomolecular Chemistry, 7*(2), 370–379. https://doi.org/10.1039/B812172A

Aksamija, A., Tomao, V., Dangles, O., & Plasson, R. (2022). Encapsulation of phenolic acids into cyclodextrins: A global statistical analysis of the effects of pH, temperature and concentrations on binding constants measured by ACE methods. *ELECTROPHORESIS, 43*(23–24), 2290–2301. https://doi.org/10.1002/elps.202200075

Alcalde, M. A., Antelo, A., Jover, A., Meijide, F., & Tato, J. V. (2009). Solubilization of cholesterol in aqueous solution by two β-cyclodextrin dimers and a negatively charged β-cyclodextrin derivative. *Journal of Inclusion Phenomena and Macrocyclic Chemistry, 63*(3–4), 309–317. https://doi.org/10.1007/s10847-008-9524-3

Al-Soufi, W., Reija, B., Felekyan, S., Seidel, C. A. M., & Novo, M. (2008). Dynamics of supramolecular association monitored by fluorescence correlation spectroscopy. *ChemPhysChem, 9*(13), 1819–1827. https://doi.org/10.1002/cphc.200800330

Anand, R., Ottani, S., Manoli, F., Manet, I., & Monti, S. (2012). A close-up on doxorubicin binding to γ-cyclodextrin: An elucidating spectroscopic, photophysical and conformational study. *RSC Advances, 2*(6), 2346–2357. https://doi.org/10.1039/C2RA01221A

Anderson, A., Campo, A., Fulton, E., Corwin, A., Jerome, W. G., & O'Connor, M. S. (2020). 7-Ketocholesterol in disease and aging. *Redox Biology, 29*, Article 101380. https://doi.org/10.1016/j.redox.2019.101380

Anderson, A. M., Kirtadze, T., Malanga, M., Dinh, D., Barnes, C., Campo, A., Clemens, D. M., Garcia-Fandiño, R., Piñeiro, Á., & O'Connor, M. S. (2021). Cyclodextrin dimers: A versatile approach to optimizing encapsulation and their application to therapeutic extraction of toxic oxysterols. *International Journal of Pharmaceutics, 606*, Article 120522. https://doi.org/10.1016/j.ijpharm.2021.120522

Aykaç, A., Martos-Maldonado, M. C., Casas-Solvas, J. M., García-Fuentes, L., & Vargas-Berenguel, A. (2012). Binding ability properties of β-cyclodextrin dimers linked through their secondary faces towards cancer chemotherapeutic agent methotrexate. *Journal of Drug Delivery Science and Technology, 22*(3), 270–272. https://doi.org/10.1016/S1773-2247(12)50039-0

Banach, M., Stulc, T., Dent, R., & Toth, P. P. (2016). Statin non-adherence and residual cardiovascular risk: There is need for substantial improvement. *International Journal of Cardiology, 225*, 184–196. https://doi.org/10.1016/j.ijcard.2016.09.075

Berendsen, H. J. C., Postma, J. P. M., Van Gunsteren, W. F., & Hermans, J. (1981). Interaction models for water in relation to protein hydration. In B. Pullman (Ed.), *Vol. 14. Intermolecular Forces* (pp. 331–342). Netherlands: Springer. https://doi.org/10.1007/978-94-015-7658-1_21.

Berendsen, H. J. C., van der Spoel, D., & van Drunen, R. (1995). GROMACS: A message-passing parallel molecular dynamics implementation. *Computer Physics Communications, 91*(1–3), 43–56. https://doi.org/10.1016/0010-4655(95)00042-E

Bertaut, E., & Landy, D. (2014). Improving ITC studies of cyclodextrin inclusion compounds by global analysis of conventional and non-conventional experiments. *Beilstein Journal of Organic Chemistry, 10*, 2630–2641. https://doi.org/10.3762/bjoc.10.275

Blaszkiewicz, C., Bricout, H., Léonard, E., Len, C., Landy, D., Cézard, C., Djedaïni-Pilard, F., Monflier, E., & Tilloy, S. (2013). A cyclodextrin dimer as a supramolecular reaction platform for aqueous organometallic catalysis. *Chemical Communications, 49*(62), 6989. https://doi.org/10.1039/c3cc43647k

Bonomi, M., Branduardi, D., Bussi, G., Camilloni, C., Provasi, D., Raiteri, P., Donadio, D., Marinelli, F., Pietrucci, F., Broglia, R. A., & Parrinello, M. (2009). PLUMED: A portable plugin for free-energy calculations with molecular dynamics. *Computer Physics Communications, 180*(10), 1961–1972. https://doi.org/10.1016/j.cpc.2009.05.011

Bonomi, M., Bussi, G., Camilloni, C., Tribello, G. A., Banáš, P., Barducci, A., Bernetti, M., Bolhuis, P. G., Bottaro, S., Branduardi, D., Capelli, R., Carloni, P., Ceriotti, M., Cesari, A., Chen, H., Chen, W., Colizzi, F., De, S., De La Pierre, M., & The PLUMED consortium. (2019). Promoting transparency and reproducibility in enhanced molecular simulations. *Nature Methods, 16*(8). https://doi.org/10.1038/s41592-019-0506-8. Article 8.

Bouchemal, K., & Mazzaferro, S. (2012). How to conduct and interpret ITC experiments accurately for cyclodextrin–guest interactions. *Drug Discovery Today, 17*(11−12), 623–629. https://doi.org/10.1016/j.drudis.2012.01.023

Breslow, R., Greenspoon, N., Guo, T., & Zarzycki, R. (1989). Very strong binding of appropriate substrates by cyclodextrin dimers. *Journal of the American Chemical Society, 111*(21), 8296–8297. https://doi.org/10.1021/ja00203a050

Breslow, R., Halfon, S., & Zhang, B. (1995). Molecular recognition by cyclodextrin dimers. *Tetrahedron, 51*(2), 377–388. https://doi.org/10.1016/0040-4020(94)00903-8

Breslow, R., & Zhang, B. (1996). Cholesterol recognition and binding by cyclodextrin dimers. *Journal of the American Chemical Society, 118*(35), 8495–8496. https://doi.org/10.1021/ja961567b

Bussi, G., Donadio, D., & Parrinello, M. (2007). Canonical sampling through velocity rescaling. *The Journal of Chemical Physics, 126*(1), Article 014101. https://doi.org/10.1063/1.2408420

Cai, W., Sun, T., Liu, P., Chipot, C., & Shao, X. (2009). Inclusion mechanism of steroid drugs into β-cyclodextrins. Insights from free energy calculations. *The Journal of Physical Chemistry B, 113*(22), 7836–7843. https://doi.org/10.1021/jp901825w

Casas-Solvas, J. M., Quesada-Soriano, I., Carreño-Gázquez, D., Giménez-Martínez, J. J., García-Fuentes, L., & Vargas-Berenguel, A. (2011). β-Cyclodextrin dimers linked through their secondary faces with rigid spacer arms as hosts for bile salts. *Langmuir, 27*(16), 9729–9737. https://doi.org/10.1021/la201180u

Chmurski, K., Stepniak, P., & Jurczak, J. (2016). Long-chain-linked β-cyclodextrin dimers: Synthesis and relationship between reactivity and inclusion complex formation. *Carbohydrate Polymers, 138*, 8–15. https://doi.org/10.1016/j.carbpol.2015.11.054

Christoforides, E., Papaioannou, A., & Bethanis, K. (2018). Crystal structure of the inclusion complex of cholesterol in β-cyclodextrin and molecular dynamics studies. *Beilstein Journal of Organic Chemistry, 14*, 838–848. https://doi.org/10.3762/bjoc.14.69

Coisne, C., Tilloy, S., Monflier, E., Wils, D., Fenart, L., & Gosselet, F. (2016). Cyclodextrins as emerging therapeutic tools in the treatment of cholesterol-associated vascular and neurodegenerative diseases. *Molecules, 21*(12), 1748. https://doi.org/10.3390/molecules21121748

Connors, K. A. (1987). *Binding constants: The measurement of molecular complex stability*. Wiley.

Darden, T., York, D., & Pedersen, L. (1993). Particle mesh Ewald: An $N \cdot \log(N)$ method for Ewald sums in large systems. *The Journal of Chemical Physics, 98*(12), 10089–10092. https://doi.org/10.1063/1.464397

de Jong, M. R., Engbersen, J. F., Huskens, J., & Reinhoudt, D. N. (2000). Cyclodextrin dimers as receptor molecules for steroid sensors. *Chemistry (Weinheim an Der Bergstrasse, Germany), 6*(21), 4034–4040. https://doi.org/10.1002/1521-3765(20001103)6:21<4034::aid-chem4034>3.0.co;2-3

Doan, A. T. N., Doan, V. T. H., Katsuki, J., Fujii, S., Kono, H., & Sakurai, K. (2022). Dramatically increased binding constant of water-soluble cyclodextrin hyperbranched polymers: Explored with diffusion ordered NMR spectroscopy (DOSY). *ACS Omega, 7*(13), 10890–10900. https://doi.org/10.1021/acsomega.1c06194

Dodziuk, H. (2002). Rigidity versus flexibility. A review of experimental and theoretical studies pertaining to the cyclodextrin nonrigidity. *Journal of Molecular Structure, 614*(1), 33–45. https://doi.org/10.1016/S0022-2860(02)00236-3

Essmann, U., Perera, L., Berkowitz, M. L., Darden, T., Lee, H., & Pedersen, L. G. (1995). A smooth particle mesh Ewald method. *The Journal of Chemical Physics, 103*(19), 8577–8593. https://doi.org/10.1063/1.470117

Flood, K. G., Reynolds, E. R., & Snow, N. H. (2001). Determination of apparent association constants of steroid–cyclodextrin inclusion complexes using a modification of the Hummel–Dreyer method. *Journal of Chromatography A, 913*(1–2), 261–268. https://doi.org/10.1016/S0021-9673(01)00567-2

Grønlund, A., Larsen, K. G., Mathiasen, A., Nielsen, J. S., Schneider, S., & Song, M. (2018). *Fast exact k-means, k-medians and Bregman divergence clustering in 1D* (arXiv: 1701.07204). *arXiv*. http://arxiv.org/abs/1701.07204.

Harris, C. R., Millman, K. J., van der Walt, S. J., Gommers, R., Virtanen, P., Cournapeau, D., Wieser, E., Taylor, J., Berg, S., Smith, N. J., Kern, R., Picus, M., Hoyer, S., van Kerkwijk, M. H., Brett, M., Haldane, A., del Río, J. F., Wiebe, M., … Oliphant, P. (2020). Array programming with NumPy. *Nature, 585*(7825). https://doi.org/10.1038/s41586-020-2649-2. Article 7825.

Hayashi, N., Chen, R., Hiraoka, M., Ujihara, T., & Ikezaki, H. (2010). Beta-cyclodextrin/surface plasmon resonance detection system for sensing bitter-astringent taste intensity of green tea catechins. *Journal of Agricultural and Food Chemistry, 58*(14), 8351–8356. https://doi.org/10.1021/jf1012693

Hayashino, Y., Sugita, M., Arima, H., Irie, T., Kikuchi, T., & Hirata, F. (2018). Predicting the binding mode of 2-hydroxypropyl-β-cyclodextrin to cholesterol by means of the MD simulation and the 3D-RISM-KH theory. *The Journal of Physical Chemistry B, 122*(21), 5716–5725. https://doi.org/10.1021/acs.jpcb.8b02098

Hess, B., Bekker, H., Berendsen, H. J. C., & Fraaije, J. G. E. M. (1997). LINCS: A linear constraint solver for molecular simulations. *Journal of Computational Chemistry, 18*(12), 1463–1472. https://doi.org/10.1002/(SICI)1096-987X(199709)18:12<1463::AID-JCC4>3.0.CO;2-H

Hunter, J. D. (2007). Matplotlib: A 2D graphics environment. *Computing in Science & Engineering, 9*(3), 90–95. https://doi.org/10.1109/MCSE.2007.55

Jabbari, A., & Sadeghi, H. (2012). Amphiphilic cyclodextrins, synthesis, utilities and application of molecular modeling in their design. In A. D. Sezer (Ed.), *Recent advances in novel drug carrier systems*. InTech. https://doi.org/10.5772/50220.

Jankowski, C. K., Lamouroux, C., Jiménez-Estrada, M., Arseneau, S., & Wagner, B. D. (2016). Factors affecting the formation of 2:1 host:guest inclusion complexes of 2-[(R-phenyl)amine]-1,4-naphthalenediones (PAN) in β- and γ-cyclodextrins. *Molecules, 21*(11). https://doi.org/10.3390/molecules21111568. Article 11.

Katzmann, J. L., Gouni-Berthold, I., & Laufs, U. (2020). PCSK9 inhibition: Insights from clinical trials and future prospects. *Frontiers in Physiology, 11*, Article 595819. https://doi.org/10.3389/fphys.2020.595819

Kim, H., Kumar, S., Kang, D.-W., Jo, H., & Park, J.-H. (2020). Affinity-driven design of cargo-switching nanoparticles to leverage a cholesterol-rich microenvironment for atherosclerosis therapy. *ACS Nano, 14*(6), 6519–6531. https://doi.org/10.1021/acsnano.9b08216

Kritharides, L., Kus, M., Brown, A. J., Jessup, W., & Dean, R. T. (1996). Hydroxypropyl-β-cyclodextrin-mediated efflux of 7-ketocholesterol from macrophage foam cells. *Journal of Biological Chemistry, 271*(44), 27450–27455. https://doi.org/10.1074/jbc.271.44.27450

Kučáková, K., & Dolenský, B. (2020). Molecular structure study of a heptakis(2,3,6-tri-O-methyl)-β-cyclodextrin complex of cholesterol. *Steroids, 155*, Article 108555. https://doi.org/10.1016/j.steroids.2019.108555

Kurkov, S. V., & Loftsson, T. (2013). Cyclodextrins. *International Journal of Pharmaceutics, 453*(1), 167–180. https://doi.org/10.1016/j.ijpharm.2012.06.055

Lebedinskiy, K., Lobaz, V., & Jindřich, J. (2022). Preparation of β-cyclodextrin-based dimers with selectively methylated rims and their use for solubilization of tetracene. *Beilstein Journal of Organic Chemistry, 18*, 1596–1606. https://doi.org/10.3762/bjoc.18.170

Liu, Y., & Chen, Y. (2006). Cooperative binding and multiple recognition by bridged Bis(*β*-cyclodextrin)s with functional linkers. *Accounts of Chemical Research, 39*(10), 681–691. https://doi.org/10.1021/ar0502275

Loftsson, T., Saokham, P., & Sá Couto, A. R. (2019). Self-association of cyclodextrins and cyclodextrin complexes in aqueous solutions. *International Journal of Pharmaceutics, 560*, 228–234. https://doi.org/10.1016/j.ijpharm.2019.02.004

López, C. A., de Vries, A. H., & Marrink, S. J. (2011). Molecular mechanism of cyclodextrin mediated cholesterol extraction. *PLoS Computational Biology, 7*(3), Article e1002020. https://doi.org/10.1371/journal.pcbi.1002020

López, C. A., de Vries, A. H., & Marrink, S. J. (2013). Computational microscopy of cyclodextrin mediated cholesterol extraction from lipid model membranes. *Scientific Reports, 3*(1), 2071. https://doi.org/10.1038/srep02071

Malde, A. K., Zuo, L., Breeze, M., Stroet, M., Poger, D., Nair, P. C., Oostenbrink, C., & Mark, A. E. (2011). An automated force field topology builder (ATB) and repository: Version 1.0. *Journal of Chemical Theory and Computation, 7*(12), 4026–4037. https://doi.org/10.1021/ct200196m

Marconi, G., Mezzina, E., Manet, I., Manoli, F., Zambelli, B., & Monti, S. (2011). Stereoselective interaction of ketoprofen enantiomers with β-cyclodextrin: Ground state binding and photochemistry. *Photochemical & Photobiological Sciences, 10*(1), 48–59. https://doi.org/10.1039/c0pp00262c

Martinet, W., Schrijvers, D. M., Timmermans, J.-P., & Bult, H. (2008). Interactions between cell death induced by statins and 7-ketocholesterol in rabbit aorta smooth

muscle cells. *British Journal of Pharmacology, 154*(6), 1236–1246. https://doi.org/10.1038/bjp.2008.181

MathWorks—Makers of MATLAB and Simulink. (n.d.). Retrieved April 4, 2023, from https://www.mathworks.com/.

McKinney, W. (2010). Data structures for statistical computing in Python. In *Proc. of the 9th Python in science conf. (SCIPY 2010)* (pp. 56–61).

Merck and Co, Inc.. (2015). *BRIDION® (sugammadex) injection drug label*.

Miyamoto, S., & Kollman, P. A. (1992). Settle: An analytical version of the SHAKE and RATTLE algorithm for rigid water models. *Journal of Computational Chemistry, 13*(8), 952–962. https://doi.org/10.1002/jcc.540130805

Mura, P. (2014). Analytical techniques for characterization of cyclodextrin complexes in aqueous solution: A review. *Journal of Pharmaceutical and Biomedical Analysis, 101*, 238–250. https://doi.org/10.1016/j.jpba.2014.02.022

Niether, D., Kawaguchi, T., Hovancová, J., Eguchi, K., Dhont, J. K. G., Kita, R., & Wiegand, S. (2017). Role of hydrogen bonding of cyclodextrin–drug complexes probed by thermodiffusion. *Langmuir, 33*(34), 8483–8492. https://doi.org/10.1021/acs.langmuir.7b02313

Nishijo, J., Moriyama, S., & Shiota, S. (2003). Interactions of cholesterol with cyclodextrins in aqueous solution. *Chemical & Pharmaceutical Bulletin, 51*(11), 1253–1257. https://doi.org/10.1248/cpb.51.1253

Oostenbrink, C., Villa, A., Mark, A. E., & Van Gunsteren, W. F. (2004). A biomolecular force field based on the free enthalpy of hydration and solvation: The GROMOS force-field parameter sets 53A5 and 53A6. *Journal of Computational Chemistry, 25*(13), 1656–1676. https://doi.org/10.1002/jcc.20090

Parrinello, M., & Rahman, A. (1981). Polymorphic transitions in single crystals: A new molecular dynamics method. *Journal of Applied Physics, 52*(12), 7182–7190. https://doi.org/10.1063/1.328693

Peluso, P., Landy, D., Nakhle, L., Dallocchio, R., Dessì, A., Krait, S., Salgado, A., Chankvetadze, B., & Scriba, G. K. E. (2023). Isothermal titration calorimetry and molecular modeling study of the complex formation of daclatasvir by γ-cyclodextrin and trimethyl-β-cyclodextrin. *Carbohydrate Polymers, 313*, Article 120870. https://doi.org/10.1016/j.carbpol.2023.120870

Piñeiro, Á., Banquy, X., Pérez-Casas, S., Tovar, E., García, A., Villa, A., Amigo, A., Mark, A. E., & Costas, M. (2007). On the characterization of host−guest complexes: Surface tension, calorimetry, and molecular dynamics of cyclodextrins with a non-ionic surfactant. *The Journal of Physical Chemistry B, 111*(17), 4383–4392. https://doi.org/10.1021/jp0688815

Piñeiro, Á., Muñoz, E., Sabín, J., Costas, M., Bastos, M., Velázquez-Campoy, A., Garrido, P. F., Dumas, P., Ennifar, E., García-Río, L., Rial, J., Pérez, D., Fraga, P., Rodríguez, A., & Cotelo, C. (2019). AFFINImeter: A software to analyze molecular recognition processes from experimental data. *Analytical Biochemistry, 577*, 117–134. https://doi.org/10.1016/j.ab.2019.02.031

Piñeiro, Á., Pipkin, J., Antle, V., & Garcia-Fandino, R. (2022). Remdesivir interactions with sulphobutylether-β-cyclodextrins: A case study using selected substitution patterns. *Journal of Molecular Liquids, 346*, Article 117157. https://doi.org/10.1016/j.molliq.2021.117157

Puglisi, A., & Yagci, Y. (2019). Cyclodextrin-based macromolecular systems as cholesterol-mopping therapeutic agents in Niemann-Pick disease type C. *Macromolecular Rapid Communications, 40*(1), 1800557. https://doi.org/10.1002/marc.201800557

Safety and Efficacy of Intravenous Trappsol Cyclo (HPBCD) in Niemann-Pick Type C Patients from ClinicalTrials.gov. (n.d.). ClinicalTrials.Gov. Retrieved April 8, 2020, from https://clinicaltrials.gov/ct2/show/NCT02912793.

Salzano, G., Wankar, J., Ottani, S., Villemagne, B., Baulard, A. R., Willand, N., Brodin, P., Manet, I., & Gref, R. (2017). Cyclodextrin-based nanocarriers containing a synergic drug combination: A potential formulation for pulmonary administration of antitubercular drugs. *International Journal of Pharmaceutics, 531*(2), 577–587. https://doi.org/10.1016/j.ijpharm.2017.05.030

Schmid, G., .S. (2001). *Original submission—Notice of GRAS exemption for beta-cyclodextrin*. Wacker Biochem Corp.

Shuang, Y., Liao, Y., Wang, H., Wang, Y., & Li, L. (2020). Preparation and evaluation of a triazole-bridged bis(β-cyclodextrin)–bonded chiral stationary phase for HPLC. *Chirality, 32*(2), 168–184. https://doi.org/10.1002/chir.23147

Soto Tellini, V. H., Jover, A., García, J. C., Galantini, L., Meijide, F., & Tato, J. V. (2006). Thermodynamics of formation of host−guest supramolecular polymers. *Journal of the American Chemical Society, 128*(17), 5728–5734. https://doi.org/10.1021/ja0572809

Strandberg, T. E., Libby, P., & Kovanen, P. T. (2020). A tale of two therapies lipid-lowering vs. anti-inflammatory therapy: A false dichotomy? *European Heart Journal - Cardiovascular Pharmacotherapy, 7*(3), 238–241. https://doi.org/10.1093/ehjcvp/pvaa131

team, T.p.d. (2023). *pandas-dev/pandas: Pandas* [computer software]. *Zenodo.*. https://doi.org/10.5281/zenodo.7794821

Tribello, G. A., Bonomi, M., Branduardi, D., Camilloni, C., & Bussi, G. (2014). PLUMED 2: New feathers for an old bird. *Computer Physics Communications, 185*(2), 604–613. https://doi.org/10.1016/j.cpc.2013.09.018

Van Gunsteren, W. F., & Berendsen, H. J. C. (1988). A leap-frog algorithm for stochastic dynamics. *Molecular Simulation, 1*(3), 173–185. https://doi.org/10.1080/08927028808080941

Varan, G., Varan, C., Erdoğar, N., Hıncal, A. A., & Bilensoy, E. (2017). Amphiphilic cyclodextrin nanoparticles. *International Journal of Pharmaceutics, 531*(2), 457–469. https://doi.org/10.1016/j.ijpharm.2017.06.010

Voskuhl, J., Schaepe, K., & Ravoo, B. J. (2011). Enhanced chiral recognition by cyclodextrin dimers. *International Journal of Molecular Sciences, 12*(7), 4637–4646. https://doi.org/10.3390/ijms12074637

Wankar, J., Salzano, G., Pancani, E., Benkovics, G., Malanga, M., Manoli, F., Gref, R., Fenyvesi, E., & Manet, I. (2017). Efficient loading of ethionamide in cyclodextrin-based carriers offers enhanced solubility and inhibition of drug crystallization. *International Journal of Pharmaceutics, 531*(2), 568–576. https://doi.org/10.1016/j.ijpharm.2017.05.041

Wu, X. (1991). Optimal quantization by matrix searching. *Journal of Algorithms, 12*(4), 663–673. https://doi.org/10.1016/0196-6774(91)90039-2

Yu, Y., Chipot, C., Cai, W., & Shao, X. (2006). Molecular dynamics study of the inclusion of cholesterol into cyclodextrins. *The Journal of Physical Chemistry B, 110*(12), 6372–6378. https://doi.org/10.1021/jp056751a